J Appl Electrochem (2008) 38:225–229
DOI 10.1007/s10800-007-9429-7

ORIGINAL PAPER

EIS investigation of passive film formation on mild steel in oxalic acid solution

A. Ashrafi · M. A. Golozar · S. Mallakpour

Received: 22 January 2007 / Revised: 25 September 2007 / Accepted: 1 October 2007 / Published online: 12 October 2007

Abstract The properties of oxide films on mild steel formed anodically in aqueous solution containing oxalic acid were investigated by means of electrochemical impedance spectroscopy (EIS). The morphology of the passive layers at different stages of film formation was investigated using scanning electron microscopy (SEM). Passivation of mild steel in oxalic acid solution is a multi-stage process that occurs before passive layer breakdown. The influence of potential on the electrochemical behavior of the passive layer was also investigated. Depending on the passive layer potential, the EIS spectra obtained exhibited a one- or two-time constant system. This suggests the formation of either a one layer or two layer oxide film on the mild steel surface, depending on the passivation potential.

Keywords Electrochemical impedance spectroscopy · Oxalic acid · Passive layer

1 Introduction

Conductive polymers are organic polymers that exhibit conductivity in the region of semiconductors. These conductive polymers are often used as corrosion resistant coatings [1]. Most conductive polymers such as polyaniline and polypyrrole are produced by oxidative polymerization processes. Formation of conductive polymer coatings can only occur on oxidizable metals, when the electrochemical conditions can lead to passivation of the metal surface without preventing electropolymerization. It has been shown that only a few electrochemical systems can meet this requirement [2, 3]. In most studies, mineral acids such as HCl and H_2SO_4 have been used to passivate the surface of oxidizable metals before polymer coating. However, coatings produced on steel substrates in these acids have poor adhesion [4]. It has been shown that only dibasic acids such as oxalic acid can passivate the steel surface while providing adequate adhesion of polypyrrole and polyaniline. Recently electrochemical polymerization processes have been developed for the formation of strongly adherent polypyrrole and polyaniline coatings from aqueous oxalic acid solution [5–7]. In addition, mechanisms of the electrodeposition process and interphase characterization have also been investigated [8, 9]. It has been shown that in order to obtain adequate adhesion of polypyrrole or polyaniline coatings, prepassivation of the steel surface is necessary [4, 10].

The electrochemical behavior and impedance characteristics of passivated carbon steel in H_2SO_4 [11], HNO_3 [12], Na_2SO_4 [13] and borate buffer [14], solutions have also been discussed. In addition, the mechanism of the anodic dissolution of iron in oxalate solution has been studied [15, 16].

The purpose of this research is to study and clarify the electrochemical behavior of the passive state of mild carbon steel in oxalic acid solution using electrochemical impedance spectroscopy. The behavior of this passive film plays an important role in the formation of conductive polymers by electropolymerization on carbon steel substrates [2].

A. Ashrafi · M. A. Golozar (✉)
Department of Materials Engineering, Isfahan University of Technology, Isfahan 8415683111, Iran
e-mail: golozar@cc.iut.ac.ir

S. Mallakpour
Department of Chemistry, Isfahan University of Technology, Isfahan 8415683111, Iran

2 Materials and experimental techniques

The working electrodes (discs of 85 mm^2) were made from 3-mm thick mild steel plates. Samples were mounted in epoxy resin with the cross-section at one end left exposed to the electrolyte. The exposed surface of electrode was polished with emery paper up to a grade of 1200. The electrode was degreased using 3-chloroethylene, rinsed with double distilled water, washed with ethanol and then dried in air. The electrolytic cell used was a standard three electrode cell with a platinum counter electrode, saturated calomel reference electrode and steel working electrode. The test solution was prepared from analytical-grade oxalic acid (0.1 M) and double-distilled water. The pH of this solution was 1.3. All measurements were carried out at constant temperature (25 ± 2 °C).

Polarization experiments were performed using a Potentiostat/Galvanostat EG&G model 263A. Potentiodynamic experiments were conducted at scan rate of 0.166 mV s^{-1} in the range –600 to 1,250 mV.

To obtain stable specimen condition of specimen in each case, the potentiodynamic experiments were performed up to a desired potential and then held for 30 min at that potential. The surfaces of all samples were then investigated using scanning electron microscopy (SEM) (Philips model XL30).

Using the frequency response analyzer, (model 1025), electrochemical impedance spectroscopy (EIS) investigations were also performed at constant potential after stable conditions were achieved. The amplitude of the superimposed AC signal was 5 mV peak-to-peak. The frequency range selected was 100 kHz to 10 mHz.

3 Results and discussion

3.1 Thermodynamics of the iron–oxalic acid–water system

Saltykov et al [15] have established the passive behavior of Fe in the pH range 1–12. Analysis of thermodynamic equilibrium between iron and oxalate aqueous solution at a pH of 1.3 for various potentials results in the following reactions:

Reaction	Potential	
$Fe \rightarrow Fe^{2+} + 2e$	–660 mV	(1)
$Fe + HC_2O_4^- \rightarrow FeC_2O_4 + H^+ + 2e$	–522 mV	(2)
$FeC_2O_4 + H_2O \rightarrow FeOH^{2+} + HC_2O_4^- + e$	+550 mV	(3)
$Fe^{2+} \rightarrow Fe^{3+} + e$	+770 mV	(4)

3.2 Potentiodynamic experiments

A typical potentiodynamic polarization curve of mild steel in oxalic acid solution within the potential range –600 to 1,250 mV is shown in Fig. 1. The scan rate used was 0.166 mV s^{-1}. Using this figure, a corrosion potential (E_{corr}) of –570 mV was measured. From this potential, up to approximately –500 mV, typical activation polarization behavior is observed. This indicates a well-defined linear characteristic. From –500 up to 1,150 mV, three distinct passive zones are clearly seen. Two of these passive zones are metastable: the first-stage zone, with a potential range from –450 to –250 mV, and the second-stage zone, with a potential range from –100 to –50 mV. These zones correspond to current densities of 4×10^{-7} to 2×10^{-5} A cm^{-2} and 3×10^{-5} to 4×10^{-5} A cm^{-2}, respectively. Conversely, within the third-stage range of 350–1,100 mV, a stable passive zone corresponding to current density of 5×10^{-5} A cm^{-2} is visible. Similar passivation behavior has also been reported in different solutions by other researchers [16]. It must be mentioned that by increasing the scan rate, the second stage of passivation would be rendered more clear. It seems that at the first stage of passivation, a metastable passive layer is formed. By increasing the potential, this metastable passive film changes to a new passive layer, one which is also metastable. Partial dissolution of the last passive layer results in the formation of a stable passive layer at higher potential. Behavior and characterization of these passive layers at various potentials were investigated using electrochemical impedance spectroscopy.

3.3 Morphological investigation

Specimens were potentiodynamically polarized up to specific points (C, F, I, and J) indicated in Fig. 1, and then held at the constant corresponding potential until a stable surface film formed. Morphologies of these passive films were studied by SEM and are shown in Fig. 2. In the first stages of passivation, rhombohedral and needle-like passive-layer crystals are observed (Fig. 2a). By increasing the applied potential, the previously formed rhombohedral crystals grew at the expense of needle-like crystals, which dissolve (Fig. 2b). In the third stage of passivation, crystals are mainly needle-like (Fig. 2c). In the transpassive region, the crystalline passive film formed in the previous stage dissolves. Figure 2d shows a partially dissolved passive film surface corresponding to point J in Fig. 1.

3.4 Impedance characteristics of passivated mild steel

Impedance measurements were carried out under potentiostatic conditions. In each case, prior to impedance measurements, the

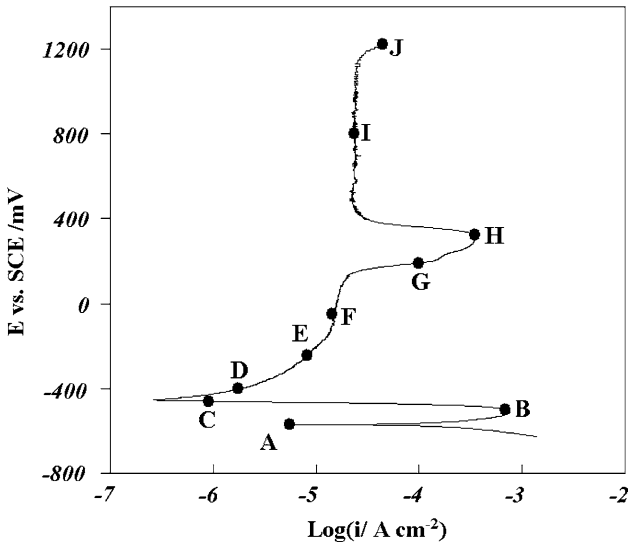

Fig. 1 Potentiodynamic polarization of mild steel in oxalic acid solution, scan rate: 0.166 mV s^{-1} (points on the graph indicate the potentials at which EIS tests were done) (A) –570 mV, (B) –500 mV, (C) –460 mV, (D) –400 mV, (E) –260 mV, (F) –50 mV, (G) 190 mV, (H) 325 mV, (I) 800 mV, (J) 1,250 mV

specimen was subjected to potentiodynamic polarization up to a desired potential then held at that potential for 30 min. Pre-determined potentials at which the impedance measurements conducted are shown in Fig. 1 (points A to J).

Figure 3 shows impedance diagrams obtained at various polarization potentials in oxalic acid solution. At point A (–570 mV), which is in the equilibrium corrosion potential region, a capacitive loop is observed. This loop indicates dissolution in the high frequency range. In this figure a relaxation behavior in the low frequency range is also observed. This figure shows a normal characteristic of metal dissolution in corroding solutions at E_{corr}. In the potential range of points B to F, –500 to –50 mV, two loops appeared in the high frequency range. These two capacitive loops may be assigned to charge transfer resistance at the metal/oxide interface and to charge transfer at the oxide/solution interface, respectively. At point E, a Warburg-like response is observed due to diffusion arising from partial dissolution of the passive layer on the metal surface. At point F, a Warburg response appears in the low frequency range. This Warburg response arises from a diffusion process and may be attributed to the charge transport in the passive film.

At point G, which is in the transition region of the passive stages, two capacitive loops were observed: one having a negative differential resistance in the low frequency range, and another in the high frequency range. This behavior is in agreement with the active–passive transition region of mild steel passivation in nitric acid reported by other researchers [12]. It is believed that, in this region, the outer layer of the passive film dissolves and a new layer forms at higher potentials. By increasing the potential, the charge transfer resistance at the oxide/solution interface reaches its minimum, point H, followed by an increase in the charge transfer resistance due to stable passive layer formation (point I).

At point J, which is in the transpassive region, dissolution of the passive layer; and a very low magnitude charge transfer resistance at oxide/solution interface is observed.

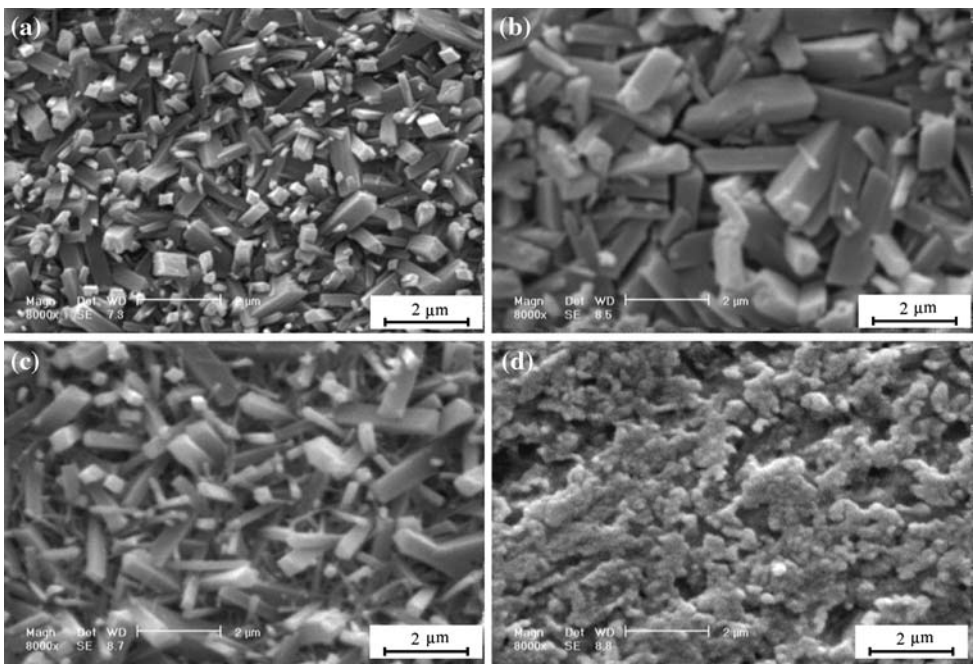

Fig. 2 SEM micrographs of mild steel surface film after potentiodynamic polarization to desired potential and potentiostatic treatment at that potentials in 0.1 M oxalic acid solution (**a**) point C –460 mV, (**b**) point F –50 mV, (**c**) point I 350 mV, (**d**) point J 1,250 mV (Refer to Fig. 1)

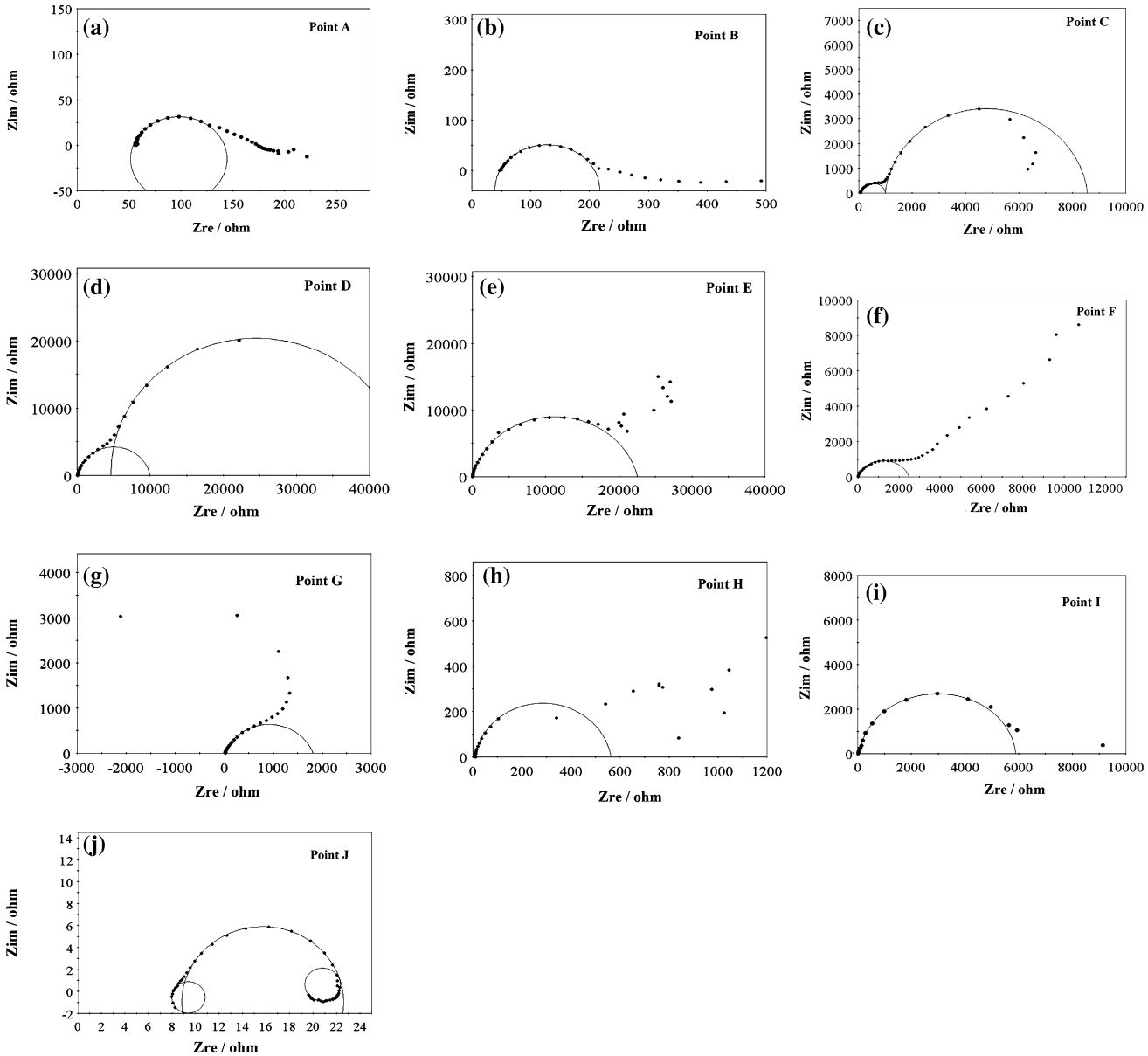

Fig. 3 EIS impedance diagrams recorded at various points indicated in Fig. 1, (A) –570 mV, (B) –500 mV, (C) –460 mV, (D) –400 mV, (E) –260 mV, (F) –50 mV, (G) 190 mV, (H) 325 mV, (I) 800 mV, (J) 1,250 mV

As the high frequency capacitive loops shown in Fig. 3 are semicircles with centers below the real axis, it can be proposed that a Cole–Cole distribution is satisfied. This is in accordance with other results [17]. The high frequency resistance (R_{HF}) includes both charge transport within the passive film and charge transfer at the passive film interface. The variation of high frequency charge transfer with the charge transfer resistance at the metal/oxide interface and oxide/solution interface is shown in Fig. 4. As demonstrated in Fig. 4a, charge transfer resistance at the metal/oxide interface increases with passive layer formation from point B to C, and reaches its maximum at point D as film formation is completed. By increasing the potential to point E, the charge transfer resistance of the metal/oxide is decreased (Fig. 4a). The same behavior is also observed for charge transfer resistance at the oxide/solution interface (Fig. 4b).

As shown in Fig. 4, R_{HF} increases with potential within the range –570 to –400 mV, but decreases at potentials above –400 mV in 0.1 M oxalic acid solution. It may be concluded that the passivation of mild steel in oxalic acid solution is largely dependent on the polarization potential. Therefore, at low over-potentials, increasing the potential impedes charge transport in the passive film and charge transfer at the passive film interfaces. After a maximum resistance (R_{HF}) at nearly –400 mV in the case of 0.1 M

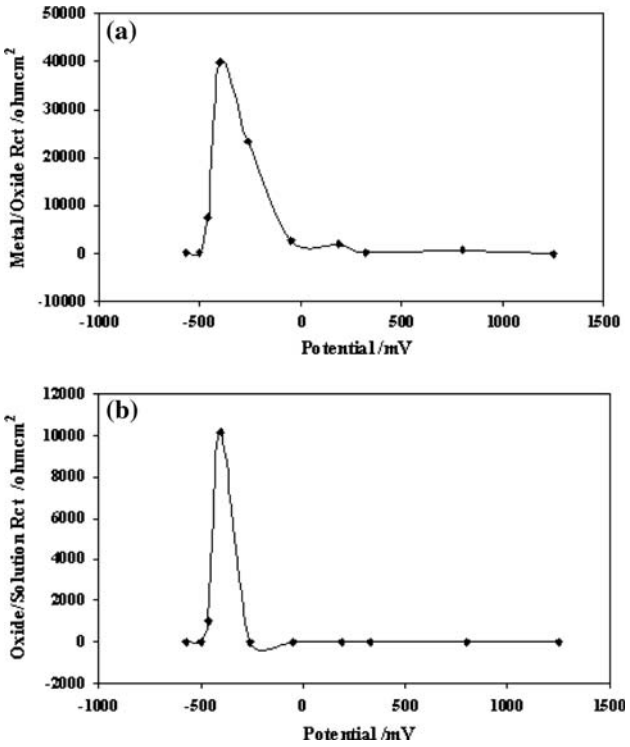

Fig. 4 Variation of charge transfer resistance of mild steel in oxalic acid solution at metal/oxide interface (**a**) and oxide/solution interface at different potentials (**b**)

oxalic acid solution, the charge transfer becomes easier as the potential is increased.

The high frequency charge transfer indicates charge transfer at passive layer interface. The passive layer formed in the initial stage of passivation has more resistance to charge transfer with respect to passive layers formed in the second and third stages.

4 Conclusions

Passive films formed potentiodynamically in 0.1 M oxalic acid solution on mild steel were investigated using SEM and EIS techniques. Passivation of mild steel in this solution occurs in three stages. The first stage results in rhombohedral and needle-like crystals. By increasing the potential in the second stage, the needle-like crystals dissolve and rhombohedral ones form. In the third stage, the passive layer has needle-like structure. EIS revealed that the passive layer formed in the first stage of passivation has maximum charge transfer resistance of any passive layer/metal or passive layer/solution interface.

Acknowledgements The authors thank the Vice Chancellor for Research and Center of Graduate Studies, Isfahan University of Technology for financial support. Editing of the manuscript by Mrs Chris Abachi and Mr Gaetano Giglione is greatly appreciated.

References

1. Ahmad N, Macdiarmid AG (1996) Synth Met 78:103
2. Su W, Iroh JO (1997) J Appl Polym Sci 65:417
3. Schirmeisen M, Beck F (1989) J Appl Electrochem 19:401
4. Sazou D, Georgoios C (1997) J Electroanal Chem 429:81
5. Su W, Iroh JO (1997) J Appl Polym Sci 65:617
6. Ashrafi A, Golozar MA, Mallakpour S (2003) Iran Polym J 12:485
7. Martyak NM, MeAndrew P, McCaskie JE, Dijon J (2002) Prog Org Coat 45:23
8. Su W, Iroh JO (1999) Electrochim Acta 44:3321
9. Su W, Iroh JO (1999) Electrochim Acta 44:4655
10. Camalet JL, Lacroix JC, Aeiyach S, Chane-Ching K, Lacaze PC (1996) J Electroanal Chem 416:179
11. Guo XP, Imaizumi H, Katoh K (1995) J Electroanal Chem 383:99
12. Guo XP, Tomoe Y, Imaizumi H, Katoh K (1998) J Electroanal Chem 445:95
13. Klyuev AL, Rotenberg ZA, Batrakov VV (2005) Russ J Electrochem 41:87
14. Hamadov L, Kadri A, Benbrahim W (2005) Appl Surf Sci 252:1510
15. Saltykov SN, Makarov GV, Toroptseva EL, Filatova YB (2004) Prot Met 40:56
16. Saltykov SN, Makarov GV, Toroptseva EL (2002) Prot Met 37:163
17. Mansfeld F, Kendig MW (1985) J Electrochem Soc 132:290